Tracking control of underactuated mechanical systems

Tracking Control of Underactuated mechanical systems

E.A.J. Geurtsen

DCT.2005.98

Coach: dr.ir N.van de Wouw
Supervisor: Prof.dr. H.Nijmeijer

EINDHOVEN UNIVERSITY OF TECHNOLOGY
DEPARTMENT OF MECHANICAL ENGINEERING
DYNAMICS AND CONTROL GROUP

Eindhoven, May 21, 2005

Summary

The interest in the control of underactuated mechanical systems has increased during the last decades. These systems are characterized by the fact that there are more degrees of freedom than actuators. Underactuated mechanical systems generate interesting control problems which require fundamentally nonlinear approaches. An H-Drive with a rotational link is such an underactuated system. For this system a state feedback controller is proposed in the literature to solve tracking problems. Moreover, an output feedback strategy using an observer is also proposed in literature. The underactuated H-Drive is controlled by a so-called 'Virtual internal model following control'. This means we opt for a controller design on different levels; namely a high-level and a low-level controller. In the current work, such a controller needs to be tested on an adapted H-Drive in the DCT-lab. First, these adaptations induce changes in the parameters of the model. Due to the new parameter settings the high-level control needs to be retuned. Moreover, the low-level controllers, concerning the tracking of the X- and Y-axes of the H-Drive, need to be redesigned. In this work, the high-level controller gains are retuned and the low-level tracking of the X- and Y-axes is redesigned. Simulations using the newly designed tracking controller show that the system is stabilized. Control performance can be improved by fine-tuning the parameters of the high-level controller. Finally conclusions are drawn and recommendations are made towards the control implementation on the adapted H-Drive manipulator.

Acknowledgments

During this project I learned a lot of new things in control theory and multibody dynamics. I have met a lot of new people who made it possible for me to realize this project, and I would like to thank a few of them: first of all Henk Nijmeijer and Nathan van de Wouw for giving me this assignment and support. Renee van der Steen and Bart Jansen for the time, interest and knowledge about the H-drive. Further I would like to thank: Maarten Steinbuch, Edo Aneke for their knowledge and previous work.

Evert Geurtsen

Contents

Chapter 1 Introduction

Underactuated mechanical systems inherit their name from the fact that there are more degrees of freedom than actuators. Examples of underactuated systems include mobile robots, surface vessels, helicopters and space robots. Underactuated mechanical systems generate interesting control problems which require fundamentally nonlinear approaches. An H-Drive with a rotational link is such an underactuated system. Several traineeships, MSc-projects and a PhD-project are performed on this system. Based on previous work performed by Aneke, see [1], in which a dynamic model and a high-level tracking controller for the H-Drive is derived, van der Steen, see [2], designed an observer in extension to the work of Aneke [1].
Jansen, see [3], has designed and realized the adaptation of the H-Drive to perform output regulation experiments. In the current work, the work done in [1] will be applied to the adapted H-drive manipulator, available in the DCT-Lab. The most significant difference with the H-Drive used in previous work is that the link is significantly larger which causes it to exhibit a higher mass and higher inertia. Moreover, this new link can be driven by an actuator. Note that this actuator is only used to compensate the friction of the link, see Jansen [3], and is not used to control the system. In this way, the H-Drive manipulator can still be considered as a benchmark system for control design for underactuated systems. The H-Drive used in previous work is depicted in figure 1.1. The rotational link is mounted on top of the machine and is indicated with an arrow. Problems with the performance of the underactuated control were mainly due to friction in the rotational link. Therefore friction compensation is to be applied on the adapted H-Drive to deal with this problem. The adapted H-Drive is depicted in figure 1.2. The rotational link is mounted under the machine. The arrow indicates the new rotational link.

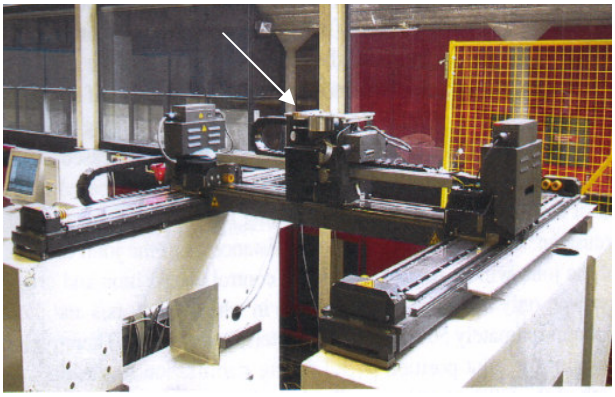

Figure 1.1: H-Drive used in previous work.

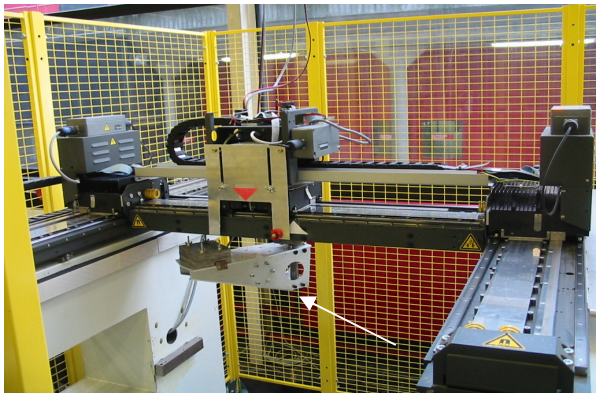

Figure 1.2: Adapted H-Drive.

Figure 1.2 shows that especially the mass and inertia of the rotational link is increased. This has consequences for the model of the H-Drive and the tuning of the control strategy used to perform tracking of the underactuated system. This will be explained in detail in this report.

1.1 Problem formulation

The tracking problems performed in previous work on the original H-Drive suffers from friction in the bearings of the rotational link. This has a negative influence on the tracking performance. On the adapted H-Drive the friction can be compensated in such a way that the tracking performance may improve significantly. The control strategy, used on the original H-Drive, need to be investigated and applied to the adapted H-Drive.

1.2 Outline of the report

This report is organized as follows. In chapter 2, the H-Drive manipulator is introduced. Here, the system will be described by a model and the parameters of the modeled system are given. In chapter 3, the control strategy will be discussed. In chapter 4, the tuning of the controllers is discussed. This subject deserves specific attention because the adapted system requires an adapted control tuning. In chapter 5, the results of the closed-loop simulations will be presented. Finally, in chapter 6 conclusions and recommendations are given.

Chapter 2 The H-Drive manipulator

In this chapter, the most important difference between the original H-Drive and the adapted H-Drive will be discussed. Moreover, the dynamics of the adapted H-Drive manipulator will be discussed. The physical parameters of the new H-Drive manipulator will be presented.

2.1 The adapted H-Drive manipulator

In the introduction, it has been explained that the control performance in previous work on the tracking control of an underactuated H-Drive suffered from friction in the rotational link. The rotational link that exhibits friction in the bearings is depicted in figure 2.1. Obviously in the adapted set-up, see figure 2.2, also friction is present in the bearings and gearbox. In this work the friction will be compensated with an actuator. The friction compensation will be based on an estimated friction model, see Jansen [3]. It should be mentioned again that the most significant difference with the H-Drive used in previous work is that the link is significantly larger which causes it to exhibit a higher mass and higher inertia.

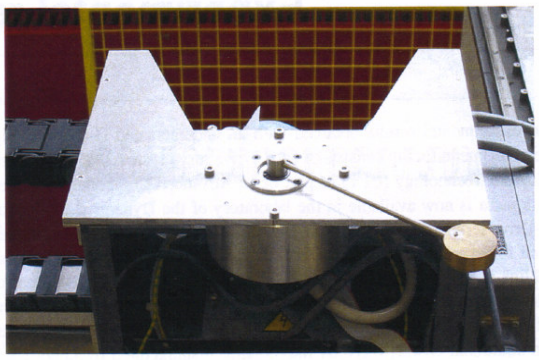

Figure 2.1: Rotational link without friction compensation.

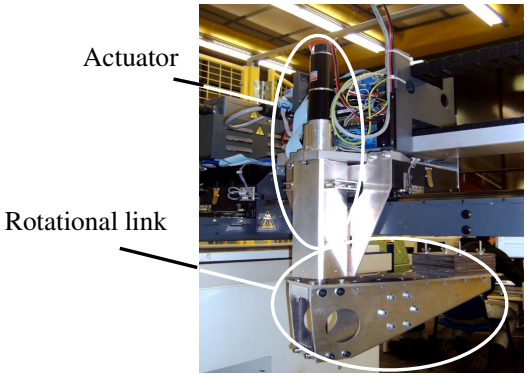

Figure 2.2: Rotational link with friction compensation.

Another difference is that the length of the rotational link has a negative effect on the area the H-Drive can operate in, see figure 2.3. The operating area is significantly smaller than on the original H-Drive. For obvious reasons the rotational link is not allowed to hit the sides of the H-Drive. This induces bounds on the operating range which have to be guaranteed by the control design.

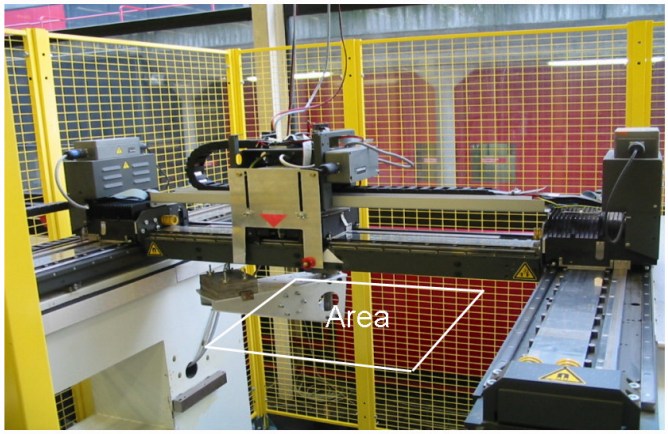

Figure 2.3: Operating area of the adapted H-Drive.

2.2 The dynamic model

A derivation of the dynamic model is given by Aneke, see [1]. A schematic representation of the H-Drive with rotational link, presented in figure 2.3, is an underactuated mechanical system with two input currents: i_X and i_Y. We use four generalized coordinates, X, Y1, Y2 and θ to describe the position of the bodies in the system. The mass of the Y-motors are denoted by m_{Y1} and m_{Y2} and the mass of the X-motor by m_X. The length of the rotational link is denoted by L; its mass and inertia by m_3 and I_3, respectively. The longitudinal forces along the Y-axes are denoted by F_{Y1} and F_{Y2}, respectively, and the transversal force along the X-axis by F_X. These forces are coupled to the input currents by the motor constants. The length of the X-axis beam is denoted by D. r_x and r_y characterize the position of the rotational link with respect to point *6* witch is the midpoint of the H-Drive, see also figure 2.3.

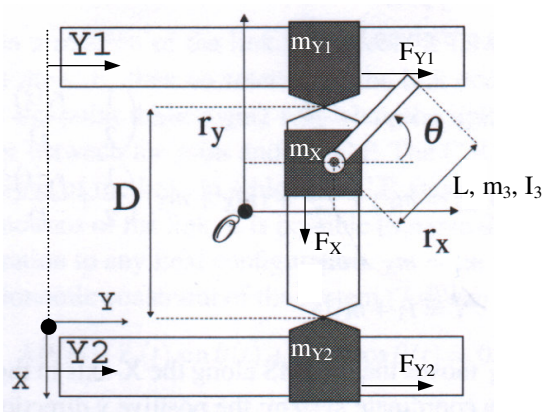

Figure 2.3: Schematic representation of the H-drive.

The relation between X, Y1, Y2 and r_x,r_y is given by a simple coordinate transformation;

$$r_x(t) = \frac{Y1(t) + Y2(t)}{2} - 0.5\,, \tag{1}$$

$$r_y(t) = -X(t) - 0.3\,. \tag{2}$$

This transformation is introduced because in previous work both sets of coordinates X, Y1, Y2, θ and r_x,r_y, θ are used to describe the dynamics of the system. It appears to be easier to formulate the model of the H-Drive in the generalized coordinates, X, Y1, Y2 and θ. So no adjustments are made to the model. The trajectories that need to be tracked are more easily formulated in the r_x and r_y coordinates.

In the table below an overview of the coordinates, inputs and parameters is given:

Description	Symbols
Generalized coordinates	X
	Y1
	Y2
	θ
Mass of Y-motors	i_X
	i_Y
Mass of Y-motors	m_{Y1}
	m_{Y2}
Mass of X-motor	m_X

Description	Symbols
Mass of rotational link	m_3
Inertia of rotational link	I_3
Length of rotational link	L
Longitudinal forces	F_{Y1}
	F_{Y2}
Transversal force	F_X
Length of the X-Beam	D

Table 2.1: Coordinates, inputs and parameters.

As derived in Aneke [1], the Lagrange-Euler formulation is used to formulate the dynamic model of the H-Drive. The dynamic model can be written as,

$$M(q)\ddot{q} + h(q,\dot{q}) = \tau, \qquad \textbf{(3)}$$

where q are the generalized coordinates, M is the mass matrix, h is the column representing coriolis and centrifugal forces and τ is the input matrix. These matrices are given in appendix A. The physical parameters are explained in the next section. Note that the model is made by ignoring possible residual friction, after friction compensation, in the bearings and gearbox of the rotational link.

2.3 Parameters of the new H-Drive manipulator

The most significant difference of the adapted H-Drive with the original system is that a large amount of mass has been added. Especially the mass and inertia of the rotational link is increased. This leads to the following parameter values:

Parameters of the rotational link.		
m_3	= 5.1434 kg	mass of the rotational link (without additional mass)
L	= 0.2433 m	length of the link with respect to the center of gravity
I_3	= 0.5392 kgm^2	moment of inertia with respect to the center of gravity
Parameters of the axes.		
m_X	= 20.9650kg	mass of the X-axes (sled, motor, gearbox and link)
m_{Y1}	= 9.12 kg	mass of the Y1-LiMMS
m_{Y2}	= 9.12 kg	mass of the Y2-LiMMS
m_B	= 32.08 kg	mass of the beam of the X-axes

Table 2.2: Physical parameters.

$\lambda = I_3 / m_3 L = 0.4309$ m, is the effective length of the rotational link.
Note that these parameters are estimated values based on CAD drawings of the design of the set-up.

Chapter 3 Control strategy

In previous work, see [1], tracking problems are solved on the original H-Drive. From this work it is concluded that friction in the rotational link is a problem and limits the tracking performance. With the adapted H-Drive, with friction compensation in the rotational link, the tracking performance may be improved significantly. The tracking problem is defined by the following desired trajectory

$$\begin{aligned} r_{xd}(t) &= 0.1\cdot\cos(\omega\cdot t), & r_{xini} &= 0.1, \\ r_{yd}(t) &= 0, & r_{yini} &= 0.1, \\ \theta_d(t) &= 0, & \theta_{ini} &= 0. \end{aligned} \qquad \textbf{(4)}$$

Where $r_{xd}(t)$, $r_{yd}(t)$ and $\theta_d(t)$ are the desired trajectories for r_x, r_y and θ respectively. From this tracking problem, with initial conditions r_{xini}, r_{yini} and θ_{ini} for r_x, r_y and θ respectively, it is clear that the rotational link is not given an initial offset; $\theta_{ini} = 0$. Instead, an initial offset is given in the position of the r_y coordinate: $r_{yini} \neq 0$. During motion the orientation of the rotational link will deviate from $\theta = 0$ as the controller will aim to achieve tracking.

The control strategy used in Aneke [1] is also used to control the adapted H-Drive in this work. The so-called 'virtual internal model following control' approach is adopted. This means that the X and Y axes are not controlled directly, but by a combination of a high-level and a low-level controller as depicted in figure 3.1 is used.
When the desired trajectories would be sent directly to the low-level controllers, the desired trajectories on the axes will be followed nicely, but the orientation of the rotational link will not be controlled. Therefore the high-level control is necessary. The high-level controller will generate desired trajectories to be sent to the X and Y-axes motors such that ultimately the desired trajectory (4) can be obtained by the low-level controllers.

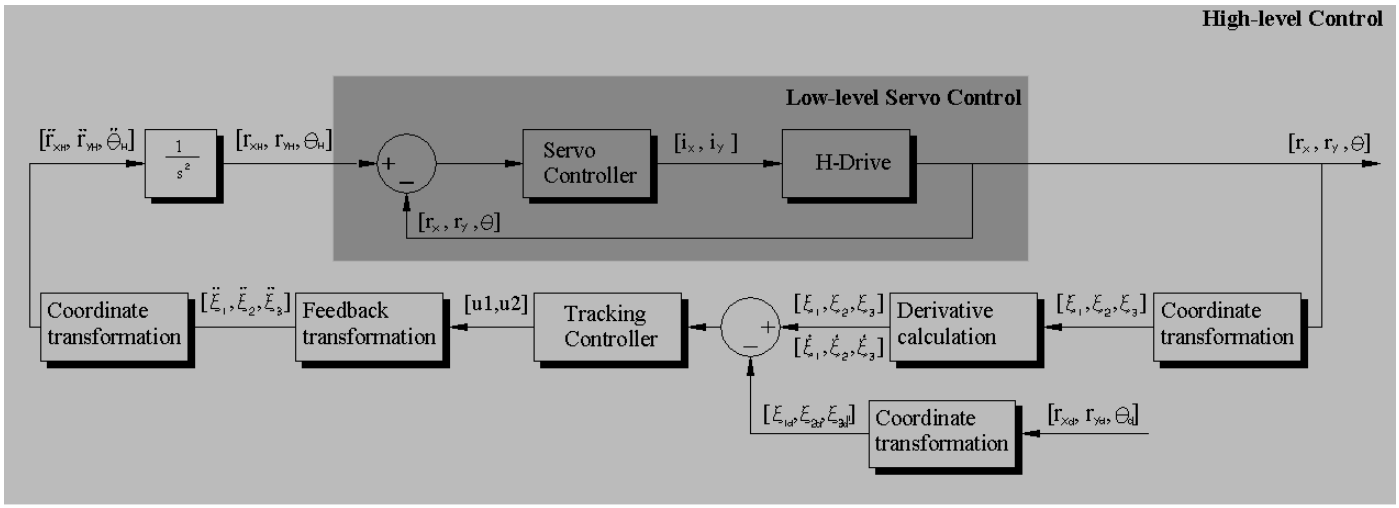

Figure 3.1: Block diagram of the H-Drive control.

The low-level servo-loop is depicted in the darker grey box, see figure 3.1. In the low-level control the H-Drive is controlled by a feedback controller. This can be seen as a normal servo controller. The output of the low-level control is send to the high-level control. First, the coordinates r_x, r_y, and θ are transformed with a coordinate transformation to a new set of coordinates ξ in order to transform the dynamics of the system into the so-called ξ-dynamics. The relation between ξ and the coordinates r_x, r_y, and θ is given by

$$\begin{aligned} \xi_1 &= r_x + \lambda(\cos(\theta) - 1), \\ \xi_2 &= \tan(\theta), \\ \xi_3 &= r_y + \lambda\sin(\theta), \end{aligned} \qquad \textbf{(5)}$$

Due to the presence of the function tan(θ) the coordinate transformation is only valid for $\theta \in [-\pi/2, \pi/2]$. Otherwise, the coordinate transformation is not well-defined since a singularity

occurs at $\theta = \pm\pi/2$. Physically this means that the rotational link may not rotate further than $\theta = \pm\pi/2$. In the design of the controllers this is a constraint that needs to be taken into account.
After the coordinate transformation the derivatives of the ξ-dynamics are calculated. The $\dot{\xi}$ are derived with the following equations

$$\begin{aligned} \dot{\xi}_1 &= \frac{\dot{Y}_1 + \dot{Y}_1}{2} - \lambda\dot{\theta}\sin\theta, \\ \dot{\xi}_2 &= \frac{\dot{\theta}}{\cos^2\theta}, \\ \dot{\xi}_3 &= -\dot{X} + \lambda\dot{\theta}\cos\theta. \end{aligned} \tag{6}$$

These equations are derivatives of the coordinate transformation given in equation (5). The ξ-dynamics and there derivatives are used in the high-level tracking controller to calculate the desired trajectories r_{XH}, r_{YH}, and θ_H for the low-level control.
The tracking controller is designed for the transformed system, which is in second-order chained form:

$$\begin{aligned} \ddot{\xi}_1 &= u_1, \\ \ddot{\xi}_2 &= u_2, \\ \ddot{\xi}_3 &= \xi_2 u_1. \end{aligned} \tag{7}$$

Formulation of the dynamics in second-order chained form is achieved by using the coordinate transformation (5). This is done to make the design of the high-level tracking controller easier. Details on the second-order chained form can be found in Aneke, see [1].
The inputs u_1 and u_2 of the second-order chained form are calculated by the high-level controller. This high-level control aims at making the ξ-variables track the desired values ξ_{1d}, ξ_{2d} and ξ_{3d}, which are computed from (4) and (5).
From these computed control actions, u_1 and u_2, the second-order derivatives of the ξ-dynamics are derived by making use of the second order chained form (7) in the feedback transformation, see figure 3.1. By making use of the inverse coordinate transformation the second-order derivatives of r_{XH}, r_{YH} and θ_H are derived. These desired accelerations are integrated twice to obtain the desired position trajectories r_{XH} and r_{YH}. These trajectories are sent to the low-level controller which aims to perform tracking of these trajectories.
Note that in the coordinate transformation and the second-order chained form the parameter λ is used. In chapter 4 the consequence of the fact that λ is changed for the adapted setup will be discussed.

3.1 Tracking controller

As explained in the previous chapter, the low-level controller can only stabilize the r_x and r_y motion. This is done by tracking the desired trajectories. The high-level controller is used to construct the desired trajectories for the low-level controllers. This should be done in such a way that tracking of the r_x and r_y motion is performed and the rotational link is also stabilized.
The design of the tracking controller in second-order chained form, see (7), is done by Aneke [1]. The derivation of this control design is not discussed in this work. However, the tuning of the gains is essential to achieve a high tracking performance and therefore this tuning process is discussed in detail in chapter 4.

In Aneke [1] the high-level tracking controller is designed as a linear time-varying tracking controller. The time-varying aspect is necessary to constantly manipulate the trajectories throughout time and eventually reach the desired trajectories despite the fact that the system is underactuated. The form of the linear time-varying tracking controller is adopted from [1] and is given by

$$\begin{aligned} u_1 &= u_{1d} - k_1(\xi_1 - \xi_{1d}) - k_2(\dot{\xi}_1 - \dot{\xi}_{1d}), \\ u_2 &= u_{2d} - G_3(t)(\xi_2 - \xi_{2d}) - G_4(t)(\dot{\xi}_2 - \dot{\xi}_{2d}) - G_5(t)(\xi_3 - \xi_{3d})G_6(t)(\dot{\xi}_3 - \dot{\xi}_{3d}), \end{aligned} \tag{8}$$

where u_{1d} and u_{2d} provide the desired trajectories through the feedback and coordinate transformation. k_1 and k_2 are time independent gains operating on the errors in the ξ_1-dynamics. $G_3(t), G_4(t), G_5(t)$ and $G_6(t)$ are time varying gains that operate on the ξ_2- and ξ_3-dynamics. These gains and error-dynamics are used to construct trajectories in the high-level controller to perform tracking on both axes and stabilize the orientation of the link. The tuning of the control gains assuring stable tracking is a complex process. The time-varying feedback coefficients $G_3(t), G_4(t), G_5(t)$ and $G_6(t)$ show this complexity and are given by

$$
\begin{aligned}
G_3(t) &= k_5 k_6 u_{1d}^4(t) + (k_3 + k_4)(k_5 + k_6) u_{1d}^2(t) + (5k_5 + 3k_6)\dot{u}_{1d}(t) u_{1d}(t) + k_3 k_4, \\
G_4(t) &= (k_5 + k_6) u_{1d}^2(t) + (k_3 + k_4), \\
G_5(t) &= 2k_5 \ddot{u}_{1d}(t) + \left(3k_5 k_6 u_{1d}^2(t) + 2k_5 (k_3 + k_4)\right)\ddot{u}_{1d}(t) + 6k_5 k_6 u_{1d}(t)\dot{u}_{1d}^2(t) \\
&+ \left(3k_5 k_6 (k_3 + k_4) u_{1d}^2(t) + 2k_3 k_4 k_5\right)\dot{u}_{1d}(t) + k_3 k_4 k_5 k_6 u_{1d}^3(t), \\
G_6(t) &= (5k_5 + k_6)\ddot{u}_{1d}(t) + \left(6k_5 k_6 u_{1d}^2(t) + (k_3 + k_4)(3k_5 + k_6)\right)\dot{u}_{1d}(t) \\
&+ k_5 k_6 (k_3 + k_4) u_{1d}^3(t) + k_3 k_4 (k_5 + k_6) u_{1d}(t).
\end{aligned}
\tag{9}
$$

These gains are time-varying because the desired trajectories u_{1d} and related time derivatives are involved. k_3, k_4, k_5 and k_6 are time-independent gains. The choice of these gains influences the ξ error-dynamics see (8). This influence is rather complex and therefore a tuning-procedure is developed in chapter 4 to perform high performance tracking.

3.2 Low-level servo control

The design of the low-level controller is based on a mass decoupling theory. For the H-Drive, the decoupling means that the variation of mass on both the Y-axes is ignored. The variation is caused by the movement of the mass of mainly the motor and rotational link on the X-axis. For more details, see [1]. Recapitulating, the dynamics of the Y-axes are influenced by the position of the X-axis. This makes it possible to develop a Linear Parameter-Varying (LPV) model, for details see van der Voort [4]. However, it is assumed that the X- and Y-axes can be decoupled, which makes it possible to design PID controllers for the X- and Y-axes independently. Because both axes can be modeled as simple masses, the corresponding dynamics is described by a double integrator. The masses used are:

The mass of the total X-axis, *mX*, used to design the low-level X-controller, is:

$$mX = m_X + m_3 \qquad = 20.96 \text{ kg} \qquad \textbf{(10)}$$

m_X = mass of the motor on the X-axis

m_3 = mass of the rotational link

The mass of the total Y-axis, *mY*, used to design both low-level Y-controllers is:

$$mY = \frac{mX}{2} + \frac{m_b}{2} + \frac{m_{Y1} + m_{Y2}}{2} + \frac{m_3}{2} \qquad = 38.21 \text{ kg} \qquad \textbf{(11)}$$

mX = total mass of the X-axis

m_b = mass of the cross-beam

m_{Y1}, m_{Y2} = mass of the motors on the Y-axes

Due to the increase of mass caused by the adapted design of the rotational link the influence of the position of the X-sled is larger. Therefore the PID controllers need to be more robust. The validation of the decoupling is tested by calculating the controller in the two extreme cases with the X-axis in the two extreme positions $mY = mX + \frac{m_b}{2} + \frac{m_{Y1} + m_{Y2}}{2} + \frac{m_3}{2}$ and $mY = \frac{m_b}{2} + \frac{m_{Y1} + m_{Y2}}{2} + \frac{m_3}{2}$.

Note that *mX* has in one case a large influence on the mass *mY* and in the other case no influence.

Chapter 4 Controller tuning

In the previous chapter the term λ is introduced. The adapted rotational link is significantly larger compared to the original link which causes it to exhibit a higher mass and higher inertia resulting in an increase of the term λ. The performance of the controller is influenced by this increase of λ. The tracking performance on the adapted H-Drive with the original controller gains appeared to be bad. Therefore, the gains of the controller need to be retuned. This also applies to the low-level controller.

4.1 Tracking control tuning

The tuning of the control parameters requires some effort because the parameters have to be chosen such that the closed-loop system is stable and such that the angle of the link stays between $\pm\pi/2$ and the operating area of the H-Drive is not exceeded.

At first hand the tuning procedure as described in Aneke [1] is followed. This procedure describes the tuning of the gains k_1 to k_6. It is expected that the adapted H-Drive behaves different than the original H-Drive. It is very difficult to determine which gains need to be changed and in which way. Therefore the tuning process is performed by investigating the influence of the individual gains. The controller described by (8) and (9) is researched to retrieve the influence of the individual gains.

The gains k_1 and k_2 affect the tracking of the ξ_1-dynamics, see (8). k_1 and k_2 need to be adjusted. This can be explained by the term λ in the ξ-dynamics, see (5). Hereby the change in λ affects the error-dynamics in the controller, see (8), in the following way;
$u_1 = u_{1d} - k_1\left(r_x + \lambda(\cos(\theta)-1) - r_{xd} - \lambda(\cos(\theta_d)-1)\right) - k_2\left(\dot{r}_x - \lambda\dot{\theta}\sin(\theta) - \dot{r}_{xd} + \lambda\dot{\theta}_d\sin(\theta_d)\right)$.
This equation is formed by substituting the coordinate transformation (5) into the controller (8). From this can be concluded that the error dynamics is behaving different due to the change in λ. The error dynamics is non-linear and it is therefore difficult to calculate stable values for k_1 and k_2. The values for k_1 and k_2 that provide stability and good tracking performance are achieved by performing simulations. In this way the gains are adjusted to the new ξ_1 error-dynamics. It appeared that a larger k_1 and k_2 are needed. Also by choosing these values sufficiently large it can be assured that the term u_1-u_{1d} becomes small sufficiently fast. This is needed because the fast convergence of u_1-u_{1d} is necessary for the cascaded backstepping in Aneke [1].

The gains k_3 k_4 and $k_3 + k_4$ affect the tracking of the ξ_2-dynamics. Because ξ_2 is chosen as a virtual input in the cascaded backstepping approach, the k_3,k_4 term is chosen sufficiently large. In this way the influence of that input is accounted for. The ξ_2-dynamics also correspond to the link orientation with $\tan\theta$. Because of this influence the parameters k_3,k_4 are chosen larger than for the original H-Drive. *It is chosen to react fast on the error in the orientation of the rotational link*. In this way the operating area needed to perform tracking is reduced.

The gains k_5 and k_6 determine the convergence of the ξ_3-dynamics that correspond to the coordinate r_y. By choosing these coefficients sufficiently large the convergence is guaranteed. The ξ_3-subsystem is stabilized using a backstepping procedure. Hereby ξ_2 is used as a virtual input; as a result the ξ_2-dynamics only converge after the tracking error dynamics of ξ_3 has been stabilized. However, choosing k_5 and k_6 too large may result in the link orientation passing through the singularity point $\pm\pi/2$ of the coordinate and feedback transformation.

The gain k_6 influences the ξ_3-dynamics. *This parameter influences the magnitude of the excursions that the system makes in the r_y coordinate*. k_6 is therefore chosen sufficiently large to minimize these excursions and reduce the operating area of the adapted H-Drive.

This tuning procedure resulted in the following parameters:

$k_1 = 20$	$k_3\,k_4 = 40$	$k_5 = 20$
$k_2 = 22$	$k_3+k_4 = 10$	$k_6 = 200$

4.2 Low-level control tuning

The design of the low-level controller is based on the mass decoupling theory. As told, the decoupling means that the variation of mass on both the Y-axes is ignored. The variation is caused by the movement of the mass of mainly the motor and rotational link on the X-axis. This mass in motion on the X-axis of the adapted H-Drive is increased compared to the mass in motion on the X-axis of the original H-Drive. The variation in mass acting on both the Y-axes is increased. As a result, the mass decoupling theory is less accurate. The variation in mass causes the magnitude of the minus-two slope, in a Bode representation of the actuated mass of the Y-axes, to change. This can cause instable crossover frequencies. The controllers need to guarantee stability over the whole operating range. Therefore, the PID controllers that control the X- and Y-axes of the H-Drive need to be more robust compared to the original controllers. The controllers are of the type PI Lead/Lag in series with a second-order low-pass filter. With the aid of the Matlab tool DIET the controllers are designed. These controllers are characterized by the following transfer functions,

controller of the Y-axes $C_Y(s) = \dfrac{100.8 \cdot s^2 + 2533 \cdot s + 1.194e004}{9.382e-007 \cdot s^3 + 0.002299 \cdot s^2 + s}$,

controller of the X-axis $C_X(s) = \dfrac{55.7 \cdot s^2 + 1400 \cdot s + 6597}{9.382e-007 \cdot s^3 + 0.002299 \cdot s^2 + s}$,

where $s \in \mathbb{C}$. Since the motors for the X- and Y-axes are of the same type, it can be assumed that all three motors have similar dynamics. The structure of the controllers therefore only differ in gains, since the mass in the direction of the Y-axes is larger than in the X-direction. A Bode-plot, in the frequency domain, of the two controllers is presented in figure 4.1. Details of the different control aspects are presented below the figures.

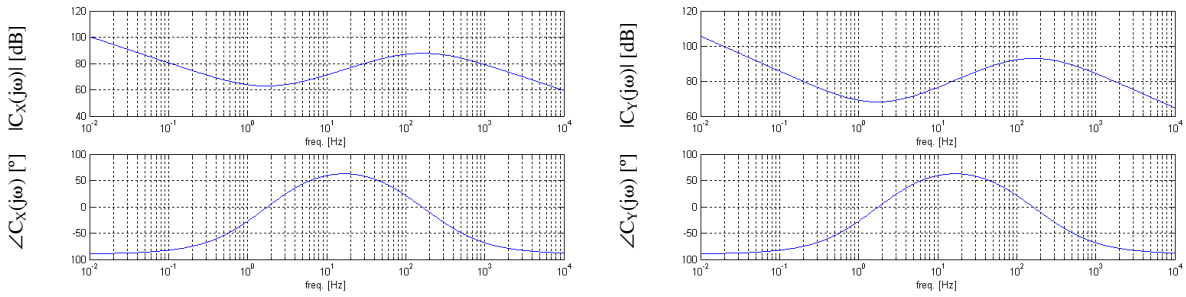

Controller x-axis

- Gain = 1050 [-]
- Integrator zero = 1 [Hz]
- Lead-Leg zero = 50/4 [Hz]
  pole = 50*4 [Hz]
- Low-pass pole = 300 [Hz]

Controller y-axis

- Gain = 1900 [-]
- Integrator zero = 1 [Hz]
- Lead-Leg zero = 50/4 [Hz]
  pole = 50*4 [Hz]
- Low-pass pole = 300 [Hz]

Figure 4.1: Bode-plot of X- and Y-axes controllers.

The resulting open-loop transfer functions are shown in figure 4.2. The controller of the X-axis has a bandwidth of around 30 [Hz] with a phase-margin of 60 [deg] and a gain margin of around 30 [dB]. The controllers of the Y-axes also have a bandwidth of around 30 [Hz] and a phase-margin of 60 [deg] and a gain margin of around 30 [dB].

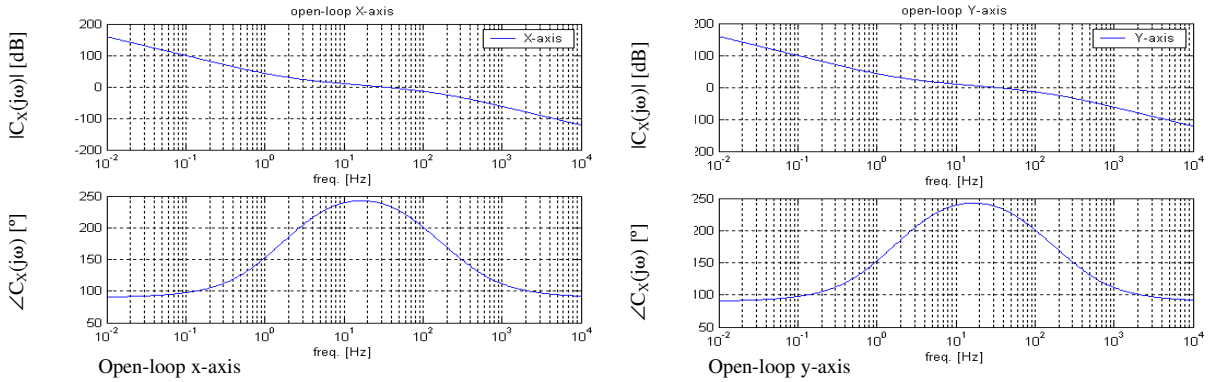

Open-loop x-axis Open-loop y-axis

Figure 4.2: Open-loop transfer of X- and Y-axes.

The two figures are in theory approximately the same. This is because the controllers only differ in gain. The design is based on decoupling. The difference in mass can therefore in theory be compensated by the gain of the controller. In practice there will be differences due to possible resonances.

Chapter 5 Closed-loop simulation

The tracking controller and the low-level controller are simulated with the aid of Matlab Simulink. Results of the closed-loop system including the retuned tracking controller are presented. The tracking of the low-level control is also evaluated.

5.1 Tracking control

The result of a simulation is presented in figure 5.1. Note that the X- and Y-coordinates are plotted instead of r_x and r_y coordinates.

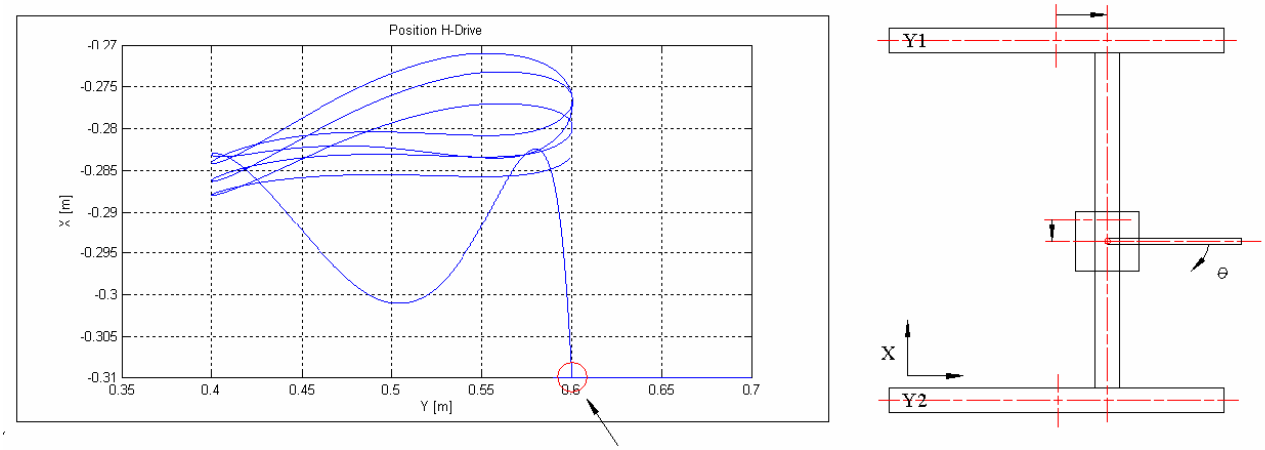

Figure 5.1: Starting position of the H-Drive manipulator.

The starting position of the H-Drive manipulator is depicted with a circle and an arrow pointing at it. On the right, the position of the H-Drive in starting position is schematically depicted. In figure 5.2, the first motion of the H-Drive is explained. It can be seen that the rotational link rotates because of the initial offset in the X-axis; this is related to the coordinate r_y . See also figure 5.3, where the rotation of the link is plotted.

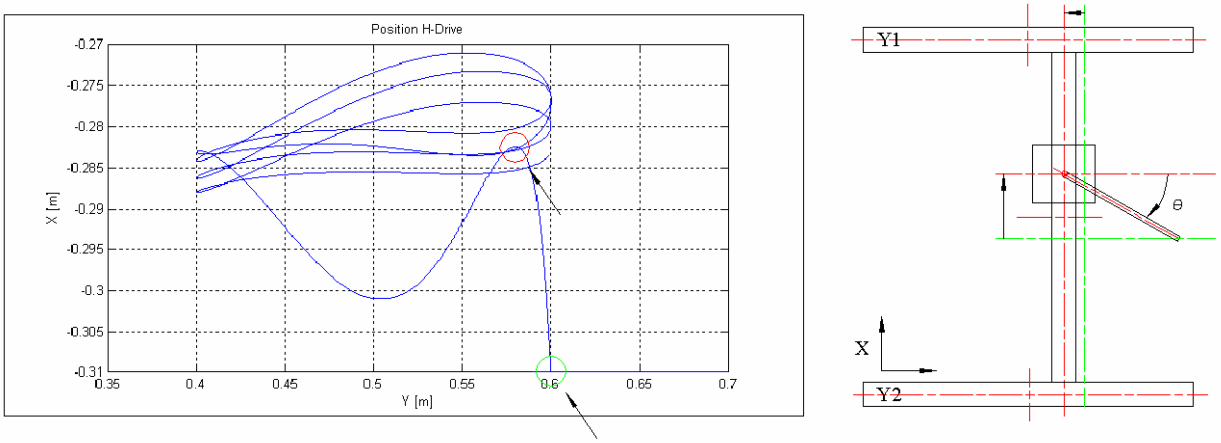

Figure 5.2: Position of the H-Drive manipulator.

In figure 5.3 the rotation of the rotational link is depicted versus time. In the figures 5.3, 5.4 and 5.5 in the first 3 seconds the system is moving towards the starting position. After these 3 seconds the tracking starts from the position depicted in figure 5.1.

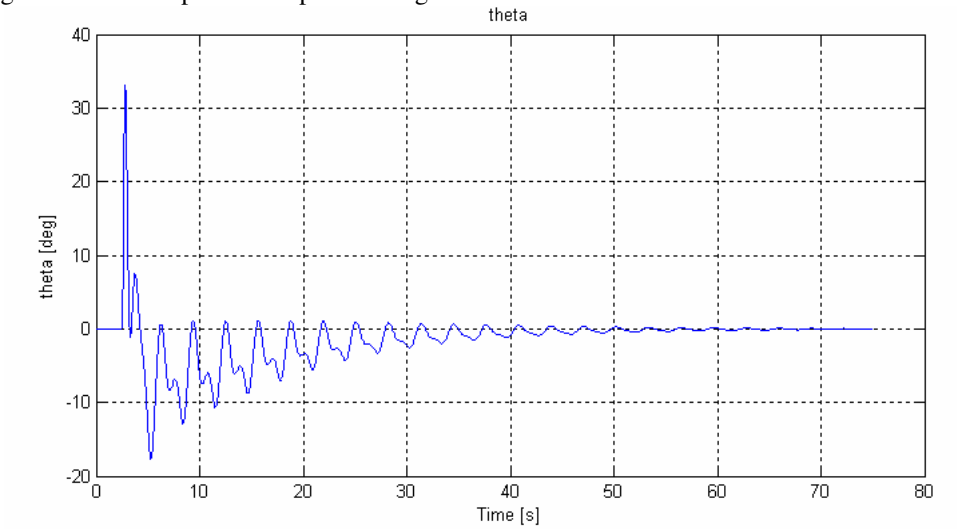

Figure 5.3: Position of rotational link.

The maximum rotation of the rotational link is 34 °. The closed-loop system is stable such that the rotational link angle stays between ± 90º. Otherwise, the coordinate transformation is not well-defined since a singularity occurs. In figure 5.4 and 5.5 the position of the X- and Y-axes are plotted.

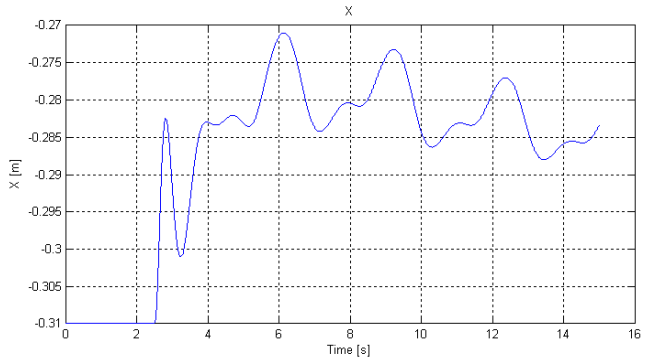

Figure 5.4: Position of the X-axis.

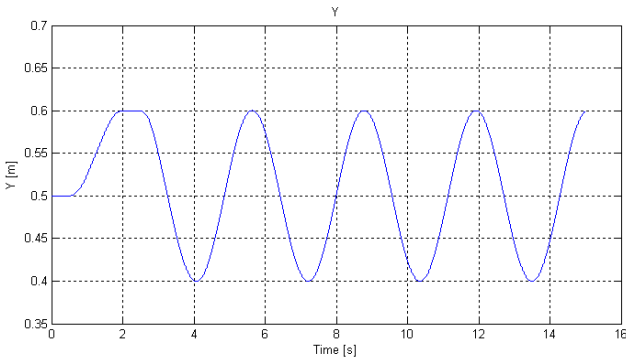

Figure 5.5: Position of the Y-axes.

Note that in figure 5.4 and 5.5 only the beginning of the motion is displayed. In this way the actual shape of the motion is better to see. From the result presented in figure 5.3 can be concluded that the stabilization is working. The stabilization is not working with fast convergence. This can be seen from the rotation of the link which is slowly converging, see figure 5.3. Also the X-axis is slowly converging, see figure 5.4. The Y-axes are performing a relative good tracking, see figure 5.5. The result is a periodic trajectory that eventually stabilizes to the desired trajectory.

5.2 Low-Level control

The low-level control is tested by taking the reference trajectory generated by the high-level control and comparing that with the realized trajectory. Note that the high-level control is not active to stabilize the rotational link. This simulation is only performed to test the low-level tracking performance. In figure 5.6 the results are displayed.

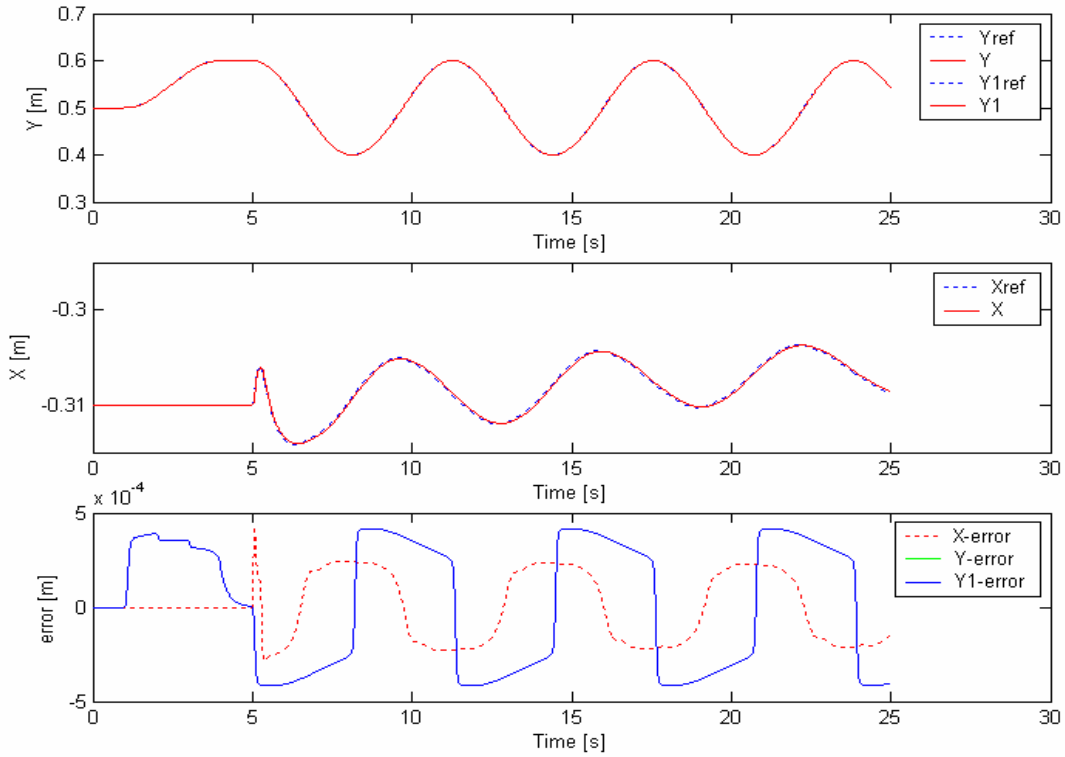

Figure 5.6: Error Low-level control.

It can be concluded that the errors are minimal. In the top figure the trajectory and the reference trajectory of both the Y-axes is displayed. Almost no difference can be seen in this figure. In the middle figure the trajectory and the reference trajectory of the X-axis is displayed. Moreover, the error on the trajectory of both axes is displayed in the last figure. The error of both the X- and Y-controller is in the order of $5 \cdot 10^{-4}$ m and is very small. From the shape of the error, it can be concluded that with feed-forward the error can be reduced even more. If we look at the Y1 error and compare this with the Y1 trajectory, there can be concluded that the error is changing sign when the motion is changing in direction. This indicates that the error is produced by accelerating and decelerating the mass of the Y-axes. By introducing a feedforward, this error can be reduced. Note that the mass on the Y-axes are varying with time, so the feedforward must be time dependent. This is optional but for this application the error is acceptable.

Chapter 6 Conclusions and Recommendations

The original H-Drive is adapted with a friction compensated rotational link in order to obtain better tracking performance. The model of the adapted H-Drive is written in the second-order chained form by a coordinate and feedback transformation. The so-called 'virtual internal model following control' approach is used to control the adapted underactuated H-Drive. In this work the low-level control is redesigned. Moreover, the high-level control is retuned. The adapted H-Drive is used to perform a tracking problem. From closed-loop simulation can be concluded that the adapted H-Drive is stable.

The Low-Level Control designed in this work is not ready to use in practice. Measurements of the FRF of the X- and Y-axes should be performed to determine possible resonances. In this way a well tuned Low-Level Control can be designed. Notches can be added to compensate for resonances.

The tracking controller can perform better. Gains of this controller can be fine-tuned to obtain improved performance. The tuning procedure described in chapter 5 may help as a guide line. The tracking controller can be tuned in such way that the same experiments can be performed as done in previous work. In this way results can be verified experimentally.

To obtain an output feedback strategy the observer can be reintroduced in the system. The gains of the observer need to be adjusted to stabilize the system. This tuning of the observer parameters will require some effort. The main goal is that the observer is faster than the controller. The tuning procedure described in chapter 5 may help as a guide line.

The simulations were performed while ignoring possible residual friction (after friction compensation) in the bearing and gearbox of the link. In future work the friction and friction compensation should be introduced and the effect on the tracking performance should be assessed.
Friction in the rotational link can be directly compensated as was done in previous work, see Jansen [3]. The friction in the X-axis can also be directly compensated. However the friction in the Y-axes needs to be identified and a compensation model needs to be made.

Appendix A

The generalized coordinates q and matrices used in the Lagrange-Euler formulation

$$M(q)\ddot{q} + h(q,\dot{q}) = \tau$$

to formulate the dynamic model of the H-Drive are given by:

$q = [X \;\; Y1 \;\; Y2 \;\; \theta]$,

$$M(q) = \begin{bmatrix} 1 & 0 & 0 & \frac{-m_3 \cdot L}{m_X + m_3} \cdot \cos\theta \\ 0 & 1 & 0 & \frac{-m_3 \cdot L}{m_{Y1} + \frac{m_3}{2}} \cdot \sin\theta \\ 0 & 0 & 1 & \frac{-m_3 \cdot L}{m_{Y2} + \frac{m_3}{2}} \cdot \sin\theta \\ -\left(\frac{1}{\lambda} \cdot \cos\theta - \frac{1}{\lambda} \cdot \sin\theta \cdot \frac{Y_2 - Y_1}{D}\right) & -\frac{1}{\lambda} \cdot \sin\theta \cdot \frac{1+X}{D} & \frac{1}{\lambda} \cdot \sin\theta \cdot \frac{X}{D} & 1 \end{bmatrix},$$

$$h(q,\dot{q}) = \begin{bmatrix} \frac{m_3 \cdot L}{m_X + m_3} \cdot \sin\theta + \dot{\theta}^2 \\ \frac{-m_3 \cdot L}{m_{Y1} + \frac{m_3}{2}} \cdot \cos\theta + \dot{\theta}^2 \\ \frac{-m_3 \cdot L}{m_{Y2} + \frac{m_3}{2}} \cdot \cos\theta + \dot{\theta}^2 \\ -\frac{1}{\lambda} \cdot \sin\theta - 2 \cdot \dot{X} \cdot \sin\theta \cdot \frac{\dot{Y}_2 - \dot{Y}_1}{D} \end{bmatrix},$$

and

$$\tau = \begin{bmatrix} \frac{F_X}{m_X + m_3} & \frac{F_{Y1}}{m_{Y1} + \frac{m_3}{2}} & \frac{F_{Y2}}{m_{Y2} + \frac{m_3}{2}} & 1 \end{bmatrix}^T \cdot$$

Bibliography

[1] N.P.I. Aneke. Control of underactueted mechanical systems. PhD thesis, Eindhoven University of Technology, 2003.

[2] R. van der Steen. Observer design for systems in second-order chained form. Technical report, Eindhoven University of Technology, 2004.

[3] B..Jansen. Output Regulation For a Nonlinear Mechanical System From Design to Experiments. Master's thesis, Eindhoven University of Technology, 2004.

[4] A. van der Voort. LPV Control Based on a Pick And Place Unit. Master's thesis, Eindhoven University of Technology, 2002.